

## ORIGINAL RESEARCH

# Identification of differential molecular characteristics and key genes between low- and high-grade serous ovarian cancer by bioinformatics analysis

Kai Meng<sup>1,2,†</sup>, Yixin Zhang<sup>1,3,†</sup>, Yuanmin Qi<sup>1,4</sup>, Chuqi Liu<sup>1,3</sup>, Mengmeng Yao<sup>1,3</sup>, Zhimin Zhang<sup>1,4</sup>, Jingyu Zhao<sup>1,3</sup>, Jinghe Cao<sup>5,\*</sup>, Yan Guo<sup>4,\*</sup>

<sup>1</sup>Collaborative Innovation Center for Birth Defect Research and Transformation of Shandong Province, Jining Medical University, 272067 Jining, Shandong, China

<sup>2</sup>Lin He's Academician Workstation of New Medicine and Clinical Translation, Jining Medical University, 272067 Jining, Shandong, China

<sup>3</sup>College of Second Clinical Medical, Jining Medical University, 272067 Jining, Shandong, China

<sup>4</sup>College of Basic Medicine, Jining Medical University, 272067 Jining, Shandong, China

<sup>5</sup>Affiliated Hospital of Jining Medical University, 272100 Jining, Shandong, China

**\*Correspondence**

guoyan@mail.jnmc.edu.cn  
(Yan Guo);  
caojinghe@126.com  
(Jinghe Cao)

† These authors contributed equally.

**Abstract**

**Background:** Serous ovarian cancer (SOC) is classified into high-grade serous ovarian cancer (HGSOC) and low-grade serous ovarian cancer (LGSOC), with HGSOC and LGSOC differing significantly in terms of clinical processes, treatment methods and treatment targets. Herein, we emphasize the importance of ongoing molecular studies to distinguish between HGSOC and LGSOC to improve treatment options for patients with these specific subtypes. **Methods:** Two gene expression profiles (GSE27651 and GSE73168) from the Gene Expression Omnibus (GEO) database were analyzed using bioinformatics methods, and Metascape and the KEGG Orthology-Based Annotation System (KOBAS) online software were used to identify differentially expressed genes (DEGs) from Kyoto Encyclopedia of Genes and Genomes (KEGG) pathways significantly enriched in HGSOC and LGSOC samples. **Results:** Our findings revealed that compared to LGSOC, HGSOC exhibited significant upregulation of 265 DEGs mainly associated with the KEGG pathway of p53 signaling and focal adhesion. Additionally, 423 significantly downregulated DEGs were mainly enriched in the KEGG pathway of the chemokine signaling pathway. Among these genes, *tumor protein p53 (TP53)*, *tumor protein p53-inducible protein 3 (TP53I3)*, *ferredoxin reductase (FDXR)*, *epidermal growth factor receptor (EGFR)* and *C-X-C motif chemokine ligand 11 (CXCL11)* were identified as key hub genes through Protein-Protein Interaction (PPI) network analysis and ovarian cancer gene and protein expression analysis. Furthermore, we explored the correlation between the expression of these 5 hub genes and various factors, including ovarian cancer prognosis, immune infiltration, ovarian cancer stage, grade, age and drug targets. **Conclusions:** This study contributes to the understanding of differential signaling molecules between HGSOC and LGSOC, facilitating the transition from a monotherapy approach to a more precise treatment strategy tailored to the specific features of each subtype. Additionally, it provides valuable insights into the differential diagnosis and detection targets for these two types of ovarian cancer.

**Keywords**

GEO database; HGSOC; LGSOC; Bioinformatics; Differentially expressed genes

## 1. Introduction

Ovarian cancer, a highly lethal gynecological cancer, is often undetected until it reaches its advanced stages due to a lack of accurate early screening methods [1]. As a result, patients with ovarian cancer typically have poor prognoses and low survival rates [2, 3]. Although the primary treatment approach involves a combination of surgical resection and chemotherapy, long-term treatment can lead to the development of resistance to targeted therapies [4, 5]. Recent research has explored the potential of using cell-free DNA methylome for early ovarian cancer detection, and the combination of hyperthermic intraperitoneal chemotherapy after interval cytoreductive surgery has shown

promise in improving the survival of patients with advanced ovarian cancer [6, 7]. Despite significant efforts in this field, the overall survival rates of ovarian cancer patients have not significantly improved, possibly due to its underlying heterogeneity. Therefore, further experimental studies are crucial to identify specific differences between different ovarian cancer subtypes and offer theoretical guidance for early diagnosis and precise treatment of ovarian cancer.

Ovarian cancer is a highly heterogeneous disease, which can be divided into epithelial ovarian cancer, germ cell ovarian cancer and sex cord-stromal ovarian cancer, with epithelial ovarian cancer (EOC) being the most prevalent, accounting for over 90% of cases. Among the EOCs, serous ovarian cancer

(SOC) is the predominant type, which can be further divided into high-grade serous ovarian cancer (HGSOC) and low-grade serous ovarian cancer (LGSOC), each having distinct clinical and molecular characteristics [8]. HGSOC is the most common histologic subtype, representing more than 70% of EOC cases [9]. As a result, most therapeutic advancements have been focused on HGSOC, with limited progress in uncommon histologic subtypes [10]. On the other hand, LGSOC constitutes approximately 10% of EOC cases [11] and exhibits a unique molecular profile compared to HGSOC. LGSOC generally has a more favorable prognosis but presents specific challenges, including diagnosis at a younger age, greater resistance to chemotherapy, and prolonged overall survival [12]. Due to the heterogeneity of ovarian cancer, different therapeutic approaches have varying effects, and the clinical impact of certain cancer-related genes in ovarian cancer treatment has been limited, prompting researchers to actively seek new and more precise anti-cancer targets tailored to different cancer subtypes.

Considering the large number of heterogeneous molecules between tumors of different histological types, we aimed to explore the molecular differences between HGSOC and LGSOC by analyzing two Gene Expression Omnibus (GEO) datasets (GSE27651 and GSE73168) using HGSOC and LGSOC samples, based on which overlapping differentially expressed genes (DEGs) were identified for further investigation. Through bioinformatics methods, we analyzed and compared the molecular functions of HGSOC and LGSOC samples, leading to the identification of key differential molecules. Collectively, the findings from this research could be valuable for instances where a diagnosis is uncertain, as it could potentially provide new detection targets and therapeutic options for distinguishing between the two types of ovarian cancers.

## 2. Materials and methods

### 2.1 Data preparation and screening of DEGs

To compare the molecular differences between HGSOC and LGSOC, we selected two GEO datasets, GSE27651 and GSE73168, and carefully selected samples from each subtype for analysis and comparison. The sample sources of GSE27651 and GSE73168 are both human. Among them, GSE27651 separated epithelial cells from rapidly frozen surgical specimens through *in vitro* laser capture microdissection [13], while GSE73168 obtained human tumor samples from patients diagnosed with advanced HGSOC and LGSOC and separated epithelial tumor cells from tumor tissues of different origins using the Magnetic Particle Sorting (MACS) system (Miltenyi Biotech) [14]. First, we conducted GEO2R analysis on the selected samples and examined gene expression changes through the volcano plot generated by the limma algorithm and the mean difference plot generated by the limma package. Then, we assessed the significance of differences between the two sample groups using the Uniform Manifold Approximation and Projection (UMAP) chart and removed samples mixed with the control group. Next, we individually screened the DEGs between

HGSOC and LGSOC samples in the two datasets, using parameters set to  $\text{adj.p.val} < 0.01$  and  $|\text{Log2FC}| > 1$ . In GSE27651, we identified a total of 12,109 DEGs, with 7383 significantly upregulated genes and 4726 significantly downregulated genes. On the other hand, GSE73168 revealed 3520 DEGs, including 1094 significantly upregulated and 2426 significantly downregulated genes. To identify common DEGs between the two datasets, we performed Venn analysis on the DEGs data using the Draw Venn Diagram online website (<http://bioinformatics.psb.ugent.be/webtools/Venn>). In the follow-up studies, we intersected these genes to obtain valuable insights into the molecular distinctions between HGSOC and LGSOC.

### 2.2 Gene ontology (GO)/Kyoto encyclopedia of genes and genomes (KEGG) analysis

After performing the Venn analysis to identify significantly upregulated/downregulated genes, we further analyzed these genes using Metascape online software [15] (<https://metascape.org/gp/index.html#/main/step1>) and the top 20 clusters were selected for display [15, 16]. Additionally, we conducted KEGG pathway enrichment analysis on the aforementioned significantly upregulated/downregulated genes using the KEGG Orthology Based Annotation System (KOBAS) online [17] (<http://bioinfo.org/kobas>). A corrected  $p$ -value  $< 0.05$  was considered to identify significantly enriched genes [17].

### 2.3 Protein-protein interaction (PPI) network analysis

The PPI regulatory network for the significantly upregulated/downregulated genes identified in the Venn analysis was constructed using the STRING online website, with a minimum required interaction score of medium confidence (0.400) [18] (<https://cn.string-db.org/>). For the upregulated genes, the network consisted of 257 nodes and 445 edges, with a highly significant PPI enrichment  $p$ -value of  $2.08 \times 10^{-13}$ . On the other hand, the network for the downregulated genes included 393 nodes and 979 edges, with an even more significant PPI enrichment  $p$ -value of less than  $1.0 \times 10^{-16}$ . Subsequently, the PPI network analysis of both upregulated and downregulated genes was performed using Cytoscape software [19]. To identify the top 10 hub genes in each network, the maximal clique centrality (MCC) algorithm from the cytoHubba plugin in Cytoscape was utilized.

### 2.4 Cancer genomics analysis

Cancer genomics analysis was performed *via* the cBioPortal online website, and selected the Ovarian Serous Cystadenocarcinoma dataset from The Cancer Genome Atlas (TCGA) PanCancer data [20]. Integrative analysis of complex cancer genomics and clinical profiles using the cBioPortal The cBio Cancer Genomics Portal: An Open Platform for Exploring Multidimensional Cancer Genomics Data (<https://www.cbioportal.org/>). We analyzed the genetic alterations of 20 hub genes in all ovarian cancer patient samples (585 patients/samples) and their correlation with the

overall survival (OS) and progression-free status (PFS) of ovarian cancer patients.

## 2.5 Expression analysis of hub genes and proteins

The GeneExpression Profiling Interactive Analysis (GEPIA) online software was used to analyze the expression of hub genes in both the TCGA and Genotype-Tissue Expression (GTEx) databases of ovarian cancer [21] (<http://gepia.cancer-pku.cn/>). The protein expression of these hub genes in ovarian tumor and normal ovarian tissues was examined using the Human protein profile analysis website, all immunohistochemical images were obtained from this website (<https://www.proteinatlas.org/>).

The immunohistochemistry method used in this website is to label the antibody with DAB (3,3'-diaminobenzidine), and the antibody combines with the corresponding antigen to produce brown staining.

## 2.6 Survival and immune infiltration assays

We used the Kaplan-Meier mapper online website to investigate the association between the expression of the 5 hub genes and OS in 1657 ovarian cancer patients and PFS in 1436 ovarian cancer patients, using a log-rank  $p < 0.05$  to determine significant correlations [22, 23] (<http://kmplot.com/analysis/index.php?p=service>).

The Tumor Immune Estimation Resource (TIMER) online website was used to analyze the correlation between hub gene expression and the abundance of immune infiltrates [24] (<https://cistrome.shinyapps.io/timer/>).

## 2.7 The university of Alabama at Birmingham cancer data analysis portal (UALCAN) database analysis

The correlation of five hub genes with cancer stage, tumor grade or age of ovarian cancer patients was analyzed through the TCGA database of the UALCAN online website [25] (<https://ualcan.path.uab.edu/>).

## 2.8 Drug target and miRNA regulatory network analysis

The Tumor Immune System Interaction database (TISIDB) allows tumor and immune system interaction analysis, which was used for this study to analyze drugs targeting the hub gene through the DrugBank database of the TISIDB online website [26] (<http://cis.hku.hk/TISIDB/index.php>). MiRNet 2.0 is a website to help users analyze the miRNA regulatory network and was employed to determine the targeted miRNA regulatory network of five hub genes separately through the miRNet 2.0 online website [27] (<https://www.mirnet.ca/>).

## 3. Results

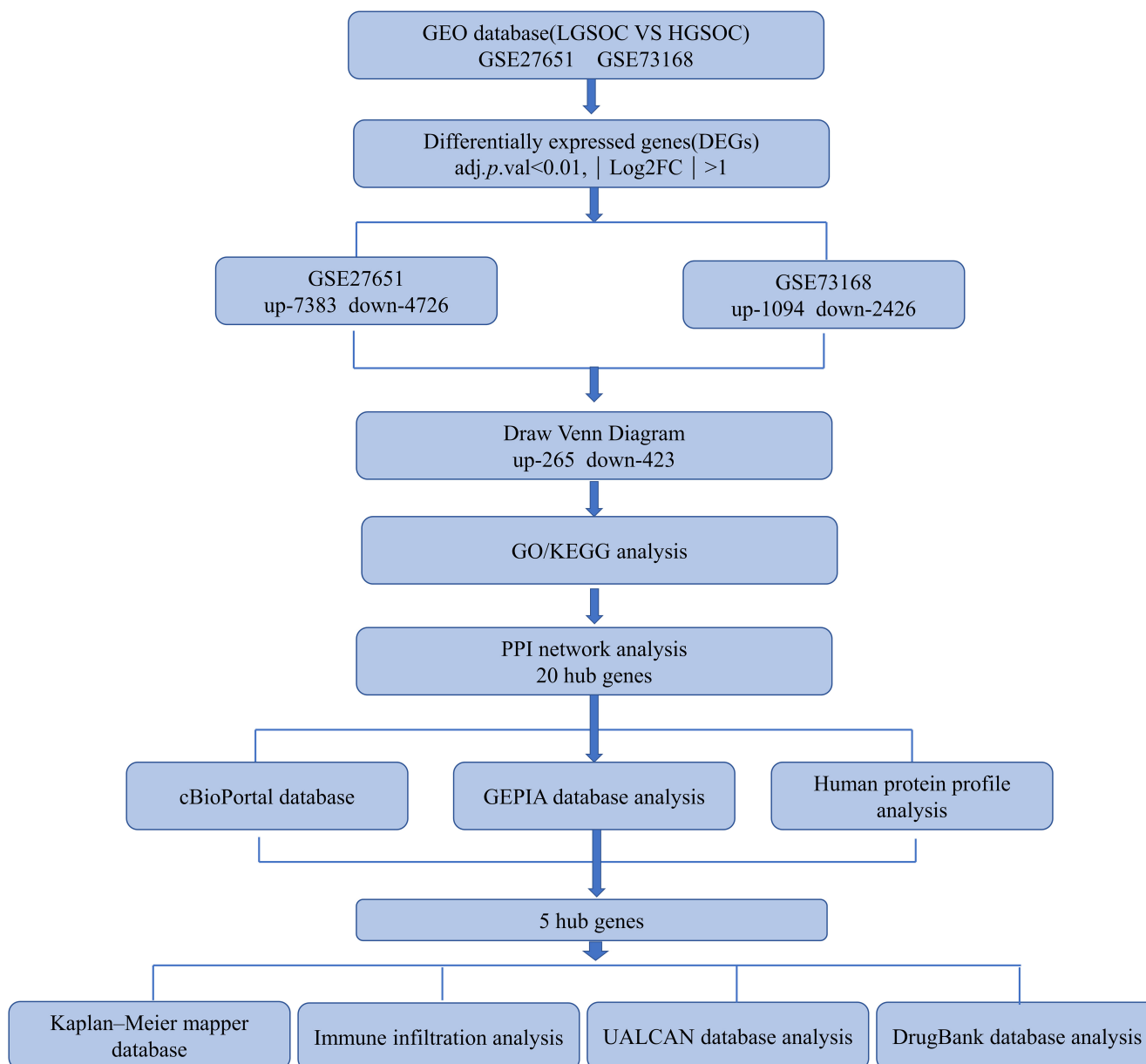
### 3.1 There were many DEGs between HGSOC and LGSOC samples

Fig. 1 presents the overall analysis process of this study. We initially analyzed the data from GSE27651 and GSE73168 through GEO2R. The volcano plot and mean difference plot demonstrated numerous DEGs between the HGSOC and LGSOC samples in both GEO datasets (Fig. 2A–D). Additionally, the UMAP plots highlighted significant overall differences in expression profiles between HGSOC and LGSOC samples (Fig. 2E,F). Subsequently, Venn analysis was performed on the DEGs from the two datasets. We found that the expression level of 265 genes in HGSOC was higher than LGSOC, and the expression level of 423 genes was lower than LGSOC. Therefore, 265 genes were upregulated and 423 genes were downregulated in HGSOC compared to LGSOC in both datasets (Fig. 2G,H). Then, we identified DEGs between HGSOC and LGSOC samples in the GSE27651 and GSE73168 datasets, and the intersected genes resulting from the Venn analysis were selected as the DEGs for further analysis.

### 3.2 GO/KEGG enrichment analysis of DEGs

In the top 20 clusters of Metascape software, we observed distinct enriched pathways and biological processes for the DEGs between HGSOC and LGSOC. For the 265 upregulated DEGs in HGSOC compared to LGSOC, the main enriched KEGG pathways were the p53 signaling pathway and focal adhesion. The main enriched GO biological processes included actin cytoskeleton organization, negative regulation of cellular component organization, negative regulation of mitotic cell cycle phase transition, regulation of cellular localization and heart development, among others. Additionally, the main enriched canonical pathway was the protein interaction domain transactivation domain of tumor protein p63 (PID TAP63) pathway, while Wiki pathways included mechano-regulation and pathology of Yes-associated protein/transcriptional coactivator with PDZ-binding motif (YAP/TAZ) *via* Hippo and non-Hippo mechanisms and Prader Willi and Angelman syndrome (Fig. 3A,B). On the other hand, for the 423 downregulated DEGs in HGSOC compared to LGSOC, the main enriched KEGG pathways were related to the Chemokine signaling pathway, pathways in cancer, and lipid and atherosclerosis. The main enriched GO biological processes included regulation of cell adhesion, immune response-regulating signaling pathway, innate immune response, response to cytokine, and response to bacterium. Furthermore, the Reactome Gene Sets analysis revealed associations with platelet activation, signaling and aggregation, with the main enriched canonical pathway being the PID T-cell receptor (TCR) pathway (Fig. 3C,D).

The results obtained from both KOBAS online software and the Metascape software were consistent, showing that the 265 upregulated DEGs were significantly enriched in the p53 signaling pathway and Focal adhesion. Furthermore, in addition to the phosphatidylinositol 3-kinases-protein kinase B (PI3K-Akt) pathway, the upregulated genes showed significant enrichment in various cancer-related pathways (Fig. 3E). On the other hand, the 423 downregulated DEGs were also significantly enriched in pathways in cancer and



**FIGURE 1. Flowchart showing the workflow for identifying DEGs, analyzing GO/KEGG pathways, and identification and functional analysis of hub genes.** GEO: Gene Expression Omnibus; GO: Gene ontology; KEGG: Kyoto Encyclopedia of genes and genomes; PPI: Protein-protein interaction; GEPIA: GeneExpression Profiling Interactive Analysis; UALCAN: university of Alabama at Birmingham cancer data analysis portal.

the chemokine signaling pathway. Additionally, besides cancer and inflammation-related pathways, the downregulated genes were enriched in pathways such as the Rap1 signaling pathway, cytokine-cytokine receptor interaction, EGFR tyrosine kinase inhibitor resistance, and the PI3K-Akt signaling pathway, among others (Fig. 3F). Based on these findings, we performed enrichment analysis on the significantly upregulated or downregulated DEGs using the Metascape software and KOBAS software, respectively, following which we identified biological processes and signaling pathways significantly enriched in these differential genes. The subsequent analyses focused on further screening hub genes playing key regulatory roles among these DEGs.

### 3.3 Screening of hub genes by PPI network construction and functional enrichment analysis

The hub genes in the PPI network were identified using the cytoHubba plugin in Cytoscape, resulting in the selection of the top 10 hub genes (Fig. 4A,B). Subsequently, we analyzed the genetic alterations of these 20 screened hub genes in ovarian cancer patients through the cBioPortal online databases, which revealed that 79.28% of the 584 cases exhibited gene alterations in ovarian cancer (Fig. 4C). Additionally, we investigated the association between cases with hub gene alterations and survival outcomes and found that alterations in the 20 hub genes were not significantly associated with OS

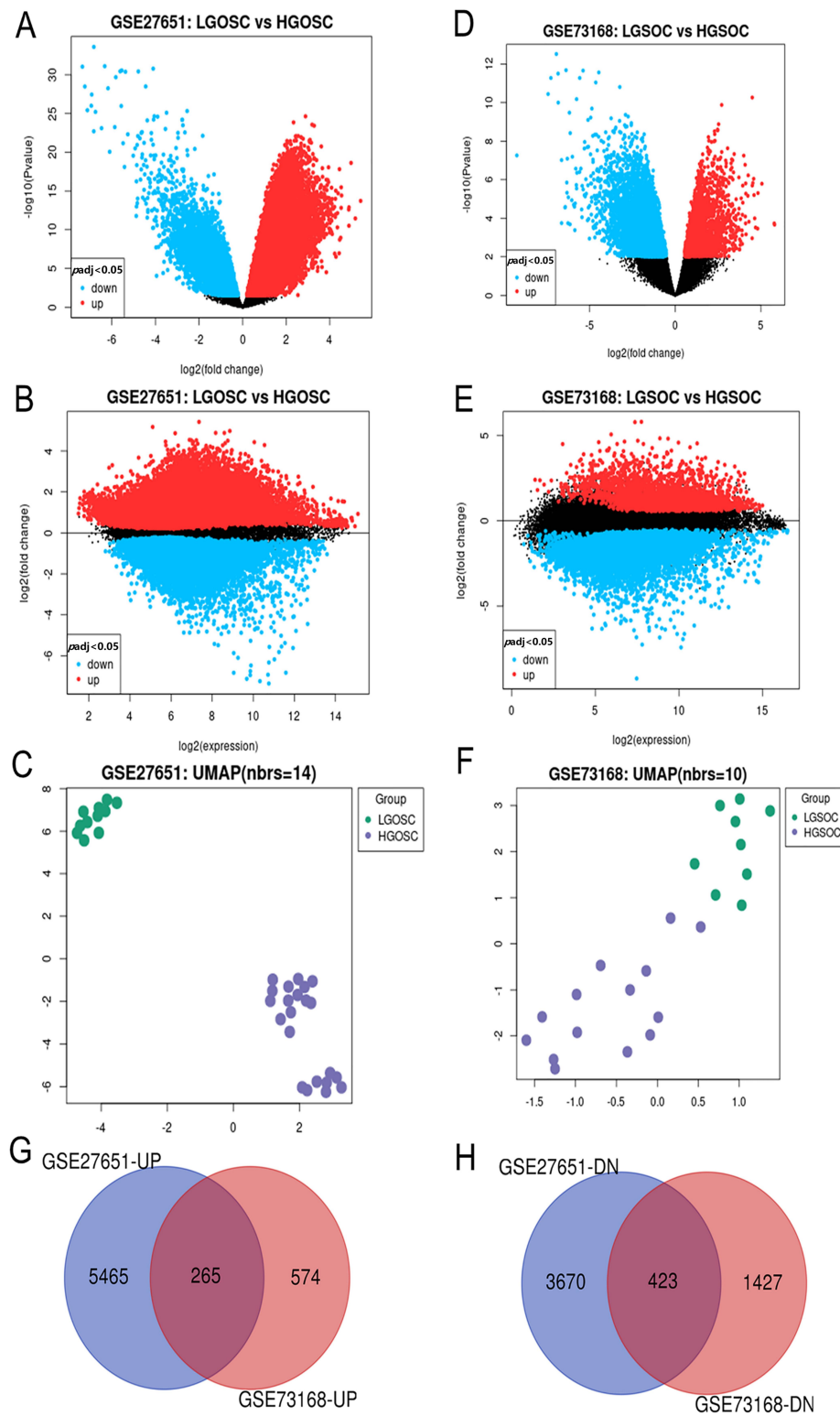


**FIGURE 2. Identification of DEGs in GSE27651 and GSE73168 from GEO datasets.** (A,B) Volcano plots of mRNA expression in GSE27651 and GSE73168. (C,D) Mean difference plot of mRNA expression in GSE27651 and GSE73168. Blue: significantly downregulated DEGs; Black: non-DEGs; Red: significantly upregulated DEGs. (E,F) UMAP plot of the sample distribution of GSE27651 and GSE73168. Green: LGSOC; Purple: HGOSC. (G,H) Venn analysis of DEGs in the two expression profiles. “Up” indicates significantly upregulated DEGs in HGOSC, and “DN” indicates significantly downregulated DEGs in HGOSC. Blue: significantly up-regulated or down-regulated genes in GSE27651; Yellow: significantly up-regulated or down-regulated genes in GSE73168. Red: Differentially expressed genes that were up-regulated or down-regulated in the two datasets and were defined as the differentially expressed genes in the subsequent analysis. HGOSC: high-grade serous ovarian cancer; LGSOC: low-grade serous ovarian cancer; UMAP: Uniform Manifold Approximation and Projection.

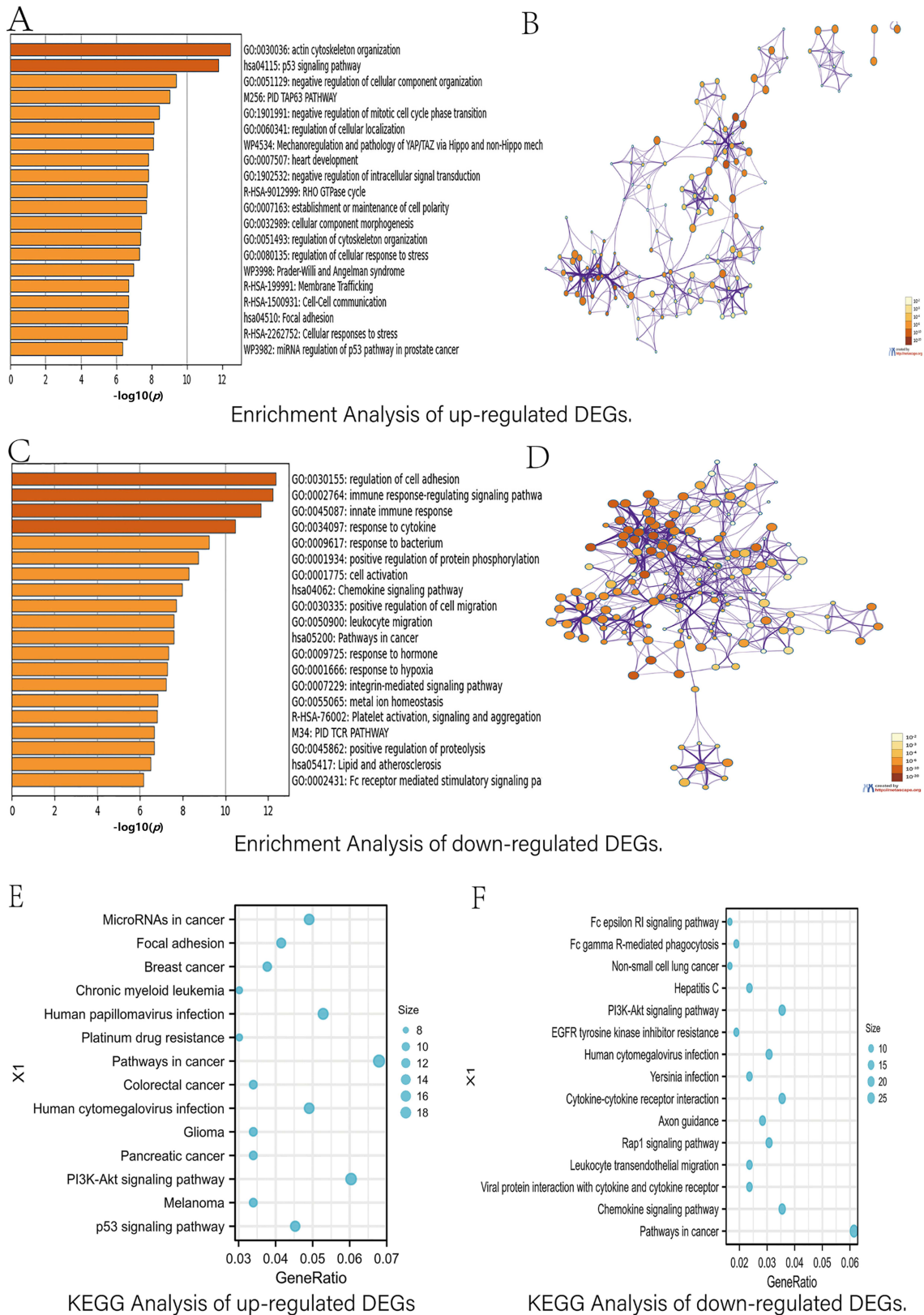


**FIGURE 3. Functional enrichment analysis of DEGs.** (A,B) Enrichment analysis of upregulated DEGs in HGSOc by Metascape software. (C,D) Enrichment analysis of downregulated DEGs in HGSOc by Metascape software. (E) KEGG analysis of upregulated DEGs in HGSOc by KOBAS software. (F) KEGG analysis of downregulated DEGs in HGSOc using the KOBAS software. PID: protein interaction domain; TAP63: transactivation domain of tumor protein p63; TCR: T-cell receptor; PI3K-Akt: phosphatidylinositol 3-kinases-protein kinase B; DEGs: differentially expressed genes; HGSOc: high-grade serous ovarian cancer; KEGG: Kyoto Encyclopedia of genes and genomes; KOBAS: KEGG Orthology-Based Annotation System; RHO GTPase: RHO guanosine triphosphatases; EGFR: epidermal growth factor receptor.

and PFS (Fig. 4D,E). The alteration frequencies of the 20 hub genes are shown in Fig. 4F. Based on the above research, we successfully screened 20 hub genes and analyzed their genetic changes and potential correlations with patient prognosis. In subsequent research, we further screened for additional hub genes playing critical roles in ovarian cancer pathogenesis and clinical outcomes.

### 3.4 Further screening of hub genes by expression analysis

We used the GEPIA online software to verify the expression of 20 hub genes. The results showed that TP53, DNA damage-binding protein 2 (DDB2), TP53I3, cyclin dependent kinase inhibitor 1A (CDKN1A), FDXR, cyclin D1 (CCND1), EGFR, C-C motif chemokine ligand 5 (CCL5), C-X-C motif chemokine ligand 10 (CXCL10), C-X-C motif chemokine receptor 4 (CXCR4), C-X-C motif chemokine receptor 3 (CXCR3) and CXCL11 were significantly different between ovarian tumor and normal tissues. Next, we analyzed the protein expression of the hub genes through representative immunohistochemical staining, and the results showed that the protein expression levels of *TP53*, *TP53I3*, *FDXR*, *EGFR* and *CXCL11* had a similar pattern of changes to the transcript levels (Fig. 5). Through GEPIA online software and protein expression analysis, we identified 5 hub genes, and in subsequent research further analyzed their relevant functions.

### 3.5 The expression of hub genes was related to the prognosis of ovarian cancer

The results of the Kaplan-Meier mapper database showed that TP53, TP53I3, FDXR and EGFR were significantly associated with PFS of ovarian cancer (Fig. 6A–D), while TP53, TP53I3, FDXR and CXCL11 were significantly associated with the OS of ovarian cancer patients (Fig. 6E–H).

### 3.6 The expression of hub genes was correlated with tumor purity and immune infiltration

The immune infiltration analysis revealed that FDXR was positively correlated with tumor purity, while EGFR and CXCL11 were negatively correlated with tumor purity. TP53 and TP53I3 showed no significant correlation with tumor purity. Additionally, *TP53* expression was positively correlated with B cell infiltration but negatively correlated with cluster of differentiation 8 positive (CD8+) T cell and macrophage infiltration. *TP53I3* expression was positively correlated with macrophage infiltration. *CXCL11* expression showed significant positive correlations with B cells, CD8+ T cells, cluster of differentiation 4 positive (CD4+) T cells, macrophage, neutrophil and dendritic cell (DC) cell infiltration. However, the expression of *FDXR* and *EGFR* did not significantly correlate with the infiltration of several immune cell types (Fig. 6I–M).

### 3.7 The expression of Hub genes was correlated with clinicopathological features of ovarian cancer

Analysis of the UALCAN database revealed that regarding cancer stage, the transcript level of *TP53I3* was significantly increased in ovarian cancer stages 2 to 3. In terms of age, *TP53* expression was significantly elevated in patients aged 81–100 years compared to patients aged 41–60 years, while the expression of *CXCL11* was significantly elevated in patients aged 41–60 years compared to patients aged 21–40 years (Fig. 7A).

### 3.8 Hub gene interacts with drugs and miRNA

Here, we identified multiple pairs of drug-gene interactions in the TISIDB online site analysis, including genes (*TP53*, *EGFR* and *FDXR*) and 34 drugs (Fig. 7B). And we analyzed and obtained the miRNA regulatory network interacting with *CXCL11*, *TP53I3*, *FDXR*, *TP53* and *EGFR* in miRNet 2.0 online website (Fig. 7C).

Through the above research, we analyzed the correlation between cancer prognosis, tumor purity, immune infiltration, clinical pathological features, drug interactions and miRNA interactions of the 5 selected hub genes. Subsequent research indicated the specific molecular mechanisms of the five hub genes.

## 4. Discussion

EOC is a heterogeneous disease, and a recent study using non-negative matrix factorization (NMF) optimally clustered 44 ovarian cancer cell lines into five distinct transcriptomes, representing five major ovarian cancer subtypes [9]. This study findings further support the classification of serous tumors into the HGSOC and LGSOC categories. A previous study comparing the immunohistochemical (IHC) expression of *breast Cancer 1 (BRCA1)*, *Ki67* and *A-catenin* in women with LGSOC and HGSOC found that *Ki67* expression was significantly higher in HGSOC [28]. LGSOC exhibits distinct epidemiological, clinical and molecular features compared to HGSOC, yet previous research has predominantly focused on HGSOC, neglecting the differences between these two subtypes. In a recent study, the impact of known clinical HGSOC prognostic factors on survival in patients with LGSOC was assessed, revealing that most known prognostic factors for HGSOC, except Federation International of Gynecology and Obstetrics (FIGO) stage and complete cytoreduction, had no effect on survival in LGSOC [29]. As research progresses and the understanding of the differences between LGSOC and HGSOC increases, these findings suggest that the same treatment strategies and standards used for high-grade disease might not be appropriate for LGSOC [30]. Thus, conducting differential studies on different subtypes of ovarian cancer can aid in transitioning ovarian cancer treatment from a one-size-fits-all approach to a more precise treatment strategy based on the specific characteristics of each subtype [31].

In this study, compared with LGSOC, we observed that the upregulated DEGs in HGSOC samples were significantly

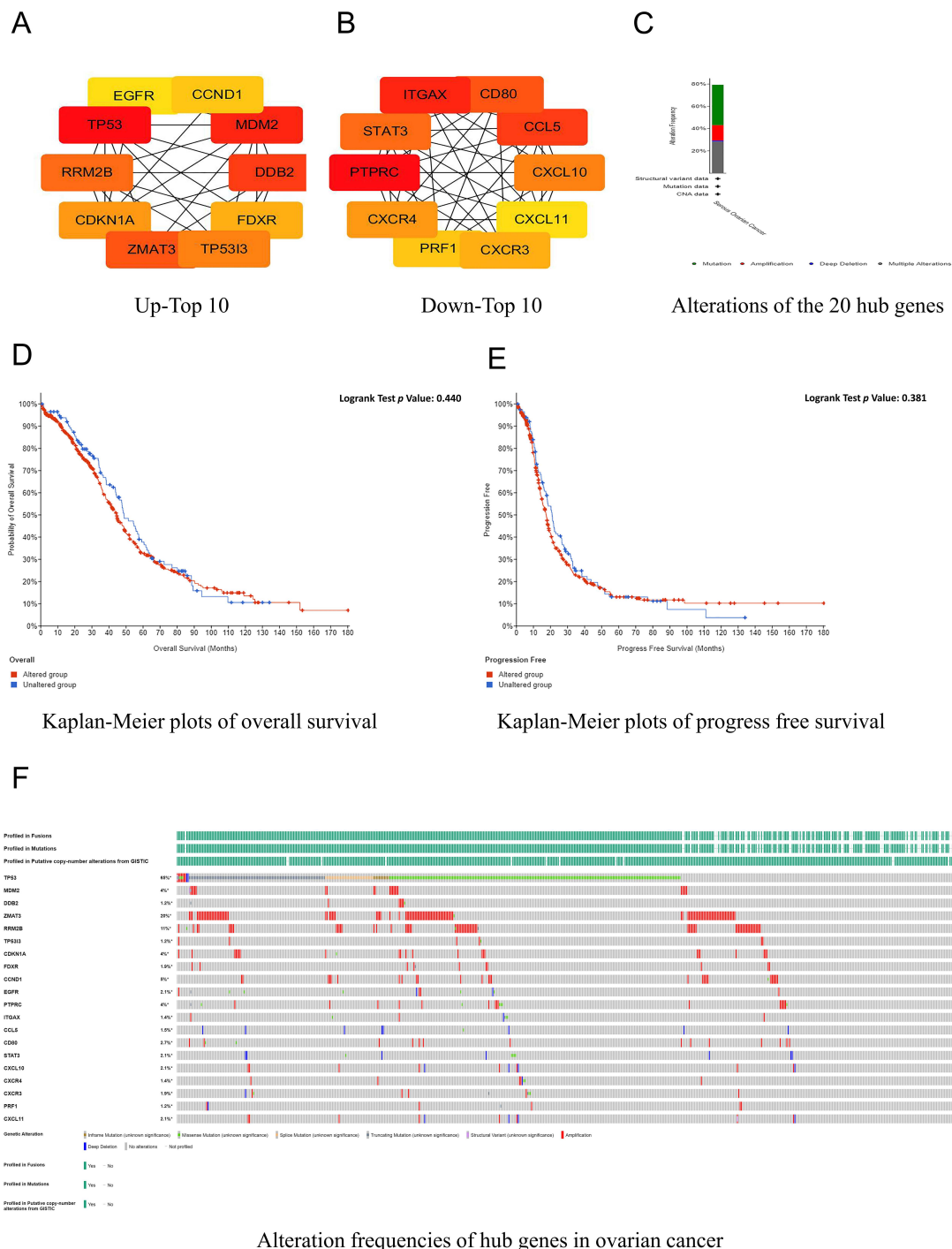


**FIGURE 4. Identification and genetic alterations of hub genes.** (A,B) The top 10 hub genes were screened using the CytoHubba plugin of the Cytoscape software. (C) Alterations of the 20 hub genes in serous ovarian cancer from the cBioPortal dataset. Green: mutation; Red: amplification; Blue: deep deletion; Gray: multiple alterations. (D) Kaplan-Meier plots of overall survival (OS) in cases with and without hub gene alterations. (E) Kaplan-Meier plots of progression-free survival (PFS) in cases with and without hub gene alterations. (F) Alteration frequencies of hub genes in ovarian cancer from the cBioPortal dataset. *EGFR*: epidermal growth factor receptor; *TP53*: tumor protein p53; *RRM2B*: ribonucleotide reductase regulatory TP53 inducible subunit M2B; *CDKN1A*: cyclin dependent kinase inhibitor 1A; *ZMAT3*: zinc finger matrin-type 3; *TP53I3*: tumor protein p53-inducible protein 3; *FDXR*: ferredoxin reductase; *DDB2*: DNA damage-binding protein 2; *MDM2*: murine double minute 2; *CCND1*: cyclin D1; *ITGAX*: integrin subunit alpha X; *STAT3*: signal transducer and activator of transcription; *PTPRC*: protein tyrosine phosphatase receptor type C; *CXCR4*: C-X-C motif chemokine receptor 4; *PRF1*: perforin-1; *CXCR3*: C-X-C motif chemokine receptor 3; *CXCL11*: C-X-C motif chemokine ligand 11; *CXCL10*: C-X-C motif chemokine ligand 10; *CCL5*: C-C motif chemokine ligand 5.



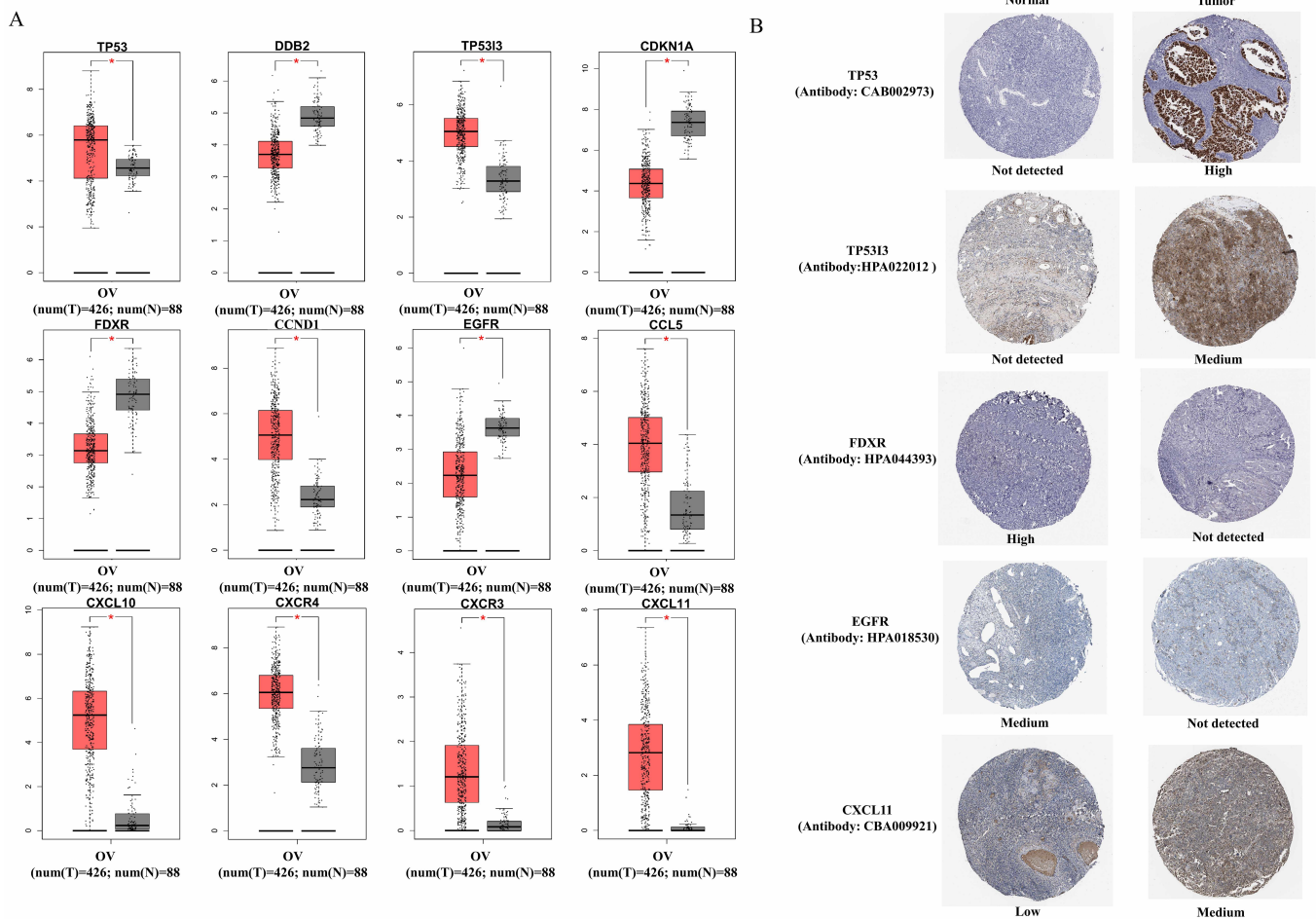


**FIGURE 5. Differential hub gene analysis and tissue immunohistochemical staining.** (A) Significantly differentially expressed hub genes between ovarian tumor and normal tissues in GEPIA. (B) Representative immunohistochemical staining of hub genes between ovarian tumor and normal tissues. OV: ovarian cancer; *TP53*: tumor protein p53; *DDB2*: Damaged-DNA binding protein 2; *TP53I3*: tumor protein p53-inducible protein 3; *CDKN1A*: cyclin dependent kinase inhibitor 1A; *FDXR*: ferredoxin reductase; *CCND1*: cyclin D1; *EGFR*: epidermal growth factor receptor; *CCL5*: C-C motif chemokine ligand 5; *CXCL10*: C-X-C motif chemokine ligand 10; *CXCR4*: C-X-C motif chemokine receptor 4; *CXCR3*: C-X-C motif chemokine receptor 3; *CXCL11*: C-X-C motif chemokine ligand 11; \*:  $p < 0.05$ .

enriched in the p53 signaling pathway and focal adhesion. *TP53*, a crucial tumor suppressor gene, is frequently altered in tumors, with about half of them having *TP53* mutations or deletions, leading to dysregulation of the p53 signaling pathway. The development of therapeutic drugs targeting the p53 pathway has been an area of active research [32]. The function of TP53 is to inhibit cell growth, and alterations in TP53 result in the loss of this negative growth regulation and a more rapid cell proliferation. Our findings suggest that there may be differences in p53 signaling pathway activity and related gene expression between the two SOC subtypes, potentially contributing to the differences in drug resistance and patient prognosis between the two subtypes. Subsequent studies could explore new differential detection targets or therapeutic agents from the p53 pathway [33]. Focal adhesion kinase (FAK), a non-receptor tyrosine kinase, is frequently activated in primary or metastatic cancers and is associated with poorer clinical outcomes [34, 35]. Focal adhesions (FAs), which are members of the Integrin adhesions family, are robust

and stable extracellular matrix contacts [36]. Previous studies have indicated that the LIM domain containing 2 (LIMD2) may promote ovarian cancer proliferation and invasion by regulating the focal adhesion signaling pathway [37]. The Fanconi anemia pathway has also been implicated in the occurrence, invasion and metastasis of ovarian cancer tumors, as well as the progression of ovarian cancer [38–42]. Our results suggest a potential molecular link between the focal adhesion signaling pathway and ovarian cancer subtypes, possibly contributing to the distinct clinical and molecular features observed in the two ovarian cancer subtypes.

Compared with LGSOC, the main enriched KEGG Pathway among the 423 downregulated DEGs in HGSOc samples was the Chemokine signaling pathway. Chemokines are a group of small proteins that interact with cell surface receptors to guide cells to specific locations [43]. Chemokines and their receptor-mediated signaling pathways play important roles in tumorigenesis and progression [44]. They are involved not only in tumor invasion but also in promoting tumor cell pro-

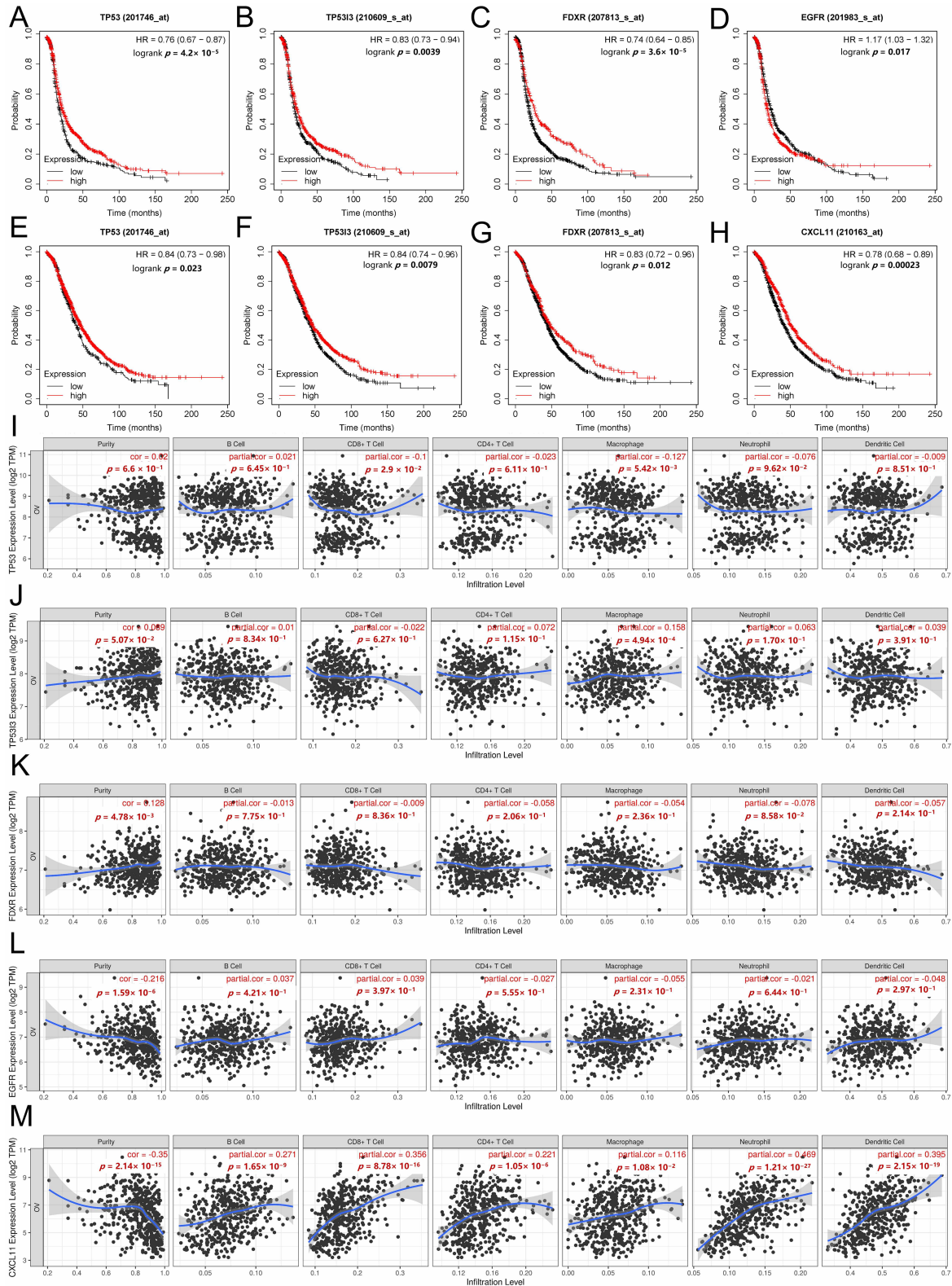


**FIGURE 6. Survival and immune infiltration analysis of five hub genes.** (A–D) Kaplan-Meier plots showing the expression of hub genes significantly associated with PFS in ovarian cancer. (E–H) Kaplan-Meier plots showing the expression of hub genes significantly associated with OS in ovarian cancer. (I–M) Correlation of the five hub genes' expression with tumor purity and B cell infiltration, CD8+ T cells, CD4+ T cells, macrophages, neutrophils, and dendritic cells in ovarian cancer. CD8+: cluster of differentiation 8 positive; CD4+: cluster of differentiation 4 positive; *TP53*: tumor protein p53; *TP53I3*: tumor protein p53-inducible protein 3; *FDXR*: ferredoxin reductase; *EGFR*: epidermal growth factor receptor; *CXCL11*: C-X-C motif chemokine ligand 11.

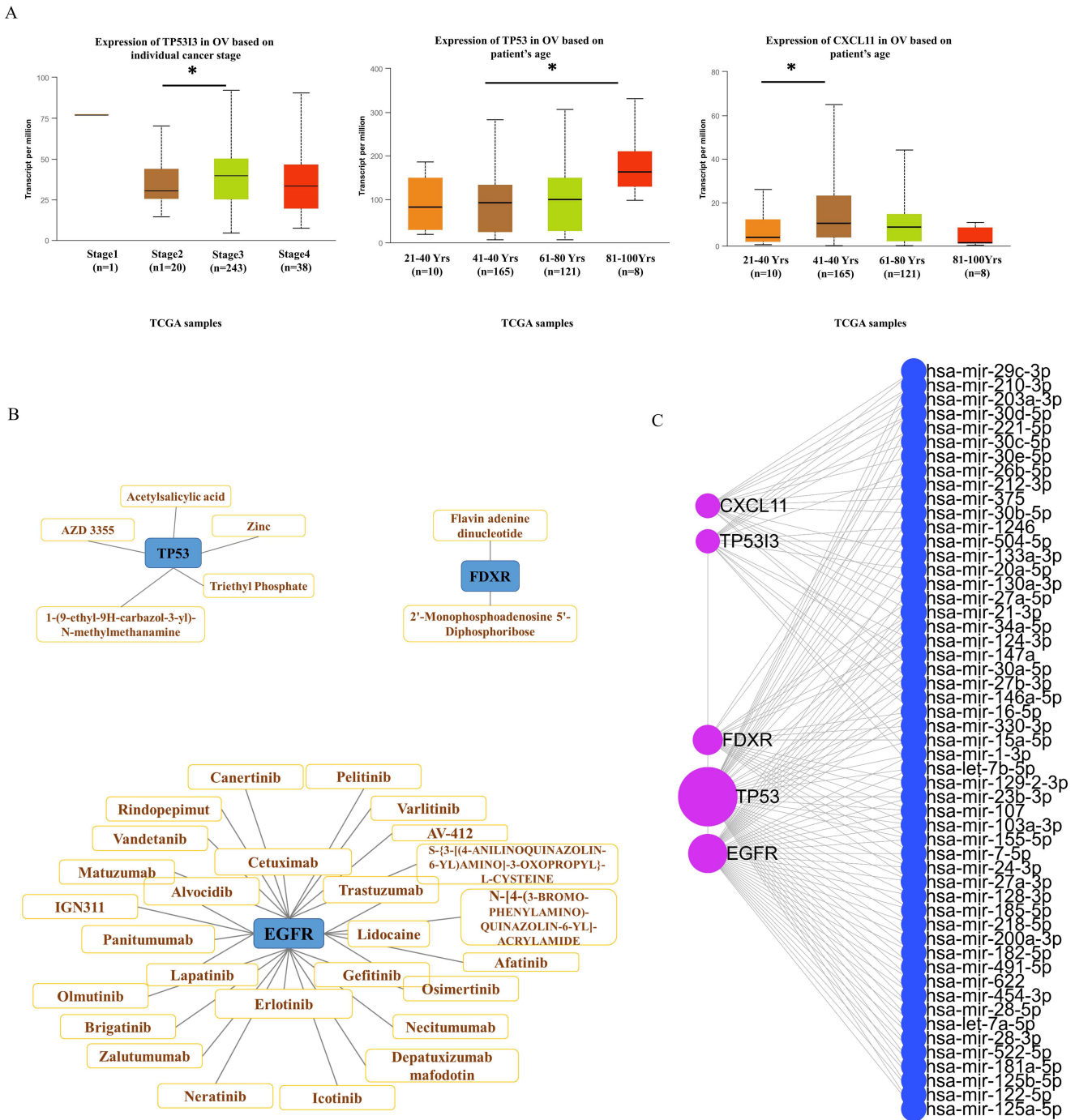


**FIGURE 7. Clinicopathological features, drug and miRNA interactions of hub genes in ovarian cancer.** (A) Correlation between the five hub genes and cancer stage, grade or age of ovarian cancer in the UALCAN database. (B) Interaction diagram of *TP53*, *EGFR*, *FDXR* and the drugs. (C) Interaction network diagram of *CXCL11*, *TP53I3*, *FDXR*, *TP53*, *EGFR* and miRNA. TCGA: The Cancer Genome Atlas; *TP53*: tumor protein p53; *TP53I3*: tumor protein p53-inducible protein 3; *FDXR*: ferredoxin reductase; *EGFR*: epidermal growth factor receptor; *CXCL11*: C-X-C motif chemokine ligand 11; \*:  $p < 0.05$ .

liferation and survival, regulating tumor cell senescence, promoting resistance to chemotherapy and endocrine therapy, and influencing the tumor microenvironment [45]. In this study, the DEGs enriched in the chemokine signaling pathway were significantly upregulated in LGSOC. Given that chemokines may promote therapeutic resistance in cancer cells, these findings could partially explain the strong resistance of LGSOC to chemotherapy.

Next, we screened out five key hub genes (*TP53*, *TP53I3*, *FDXR*, *EGFR* and *CXCL11*) through PPI network analysis and gene and protein expression analysis, and summarized the properties of these five genes (Table 1). Our results revealed that high *TP53* expression was closely associated with a favorable prognosis in ovarian cancer.

TABLE 1. Properties of the five hub genes.

Gene	Molecular functions	Expression levels compared to normal tissue	Expression levels in different subtypes	Association with ovarian cancer prognosis	Immune infiltration	Defect	Reference
<i>Tumor protein p53 (TP53)</i>	A tumor suppressor; Inhibit cell growth	Higher than normal tissues	It is higher than low-grade serous ovarian cancer (LGSOC) in high-grade serous ovarian cancer (HGSOC)	Closely associated with a favorable prognosis in ovarian cancer in terms of progression-free survival (PFS) and overall survival (OS)	Have no significant correlation with tumor purity; Positively correlated with B cell infiltration but negatively correlated with cluster of differentiation 8 positive (CD8+) T cell and macrophage infiltration	Accelerate cell proliferation; Promote multidrug resistance in ovarian cancer and an increased probability of cancer cell metastasis to the abdominal cavity	[32, 46–48]
<i>Tumor protein p53-inducible protein 3/p53 inducible gene 3 (TP53I3/PIG3)</i>	A reactive oxygen species inducer	Higher than normal tissues	It is higher than LGSOC in HGSOC	Closely associated with a favorable prognosis in ovarian cancer in terms of PFS and OS	Have no significant correlation with tumor purity; Positively correlated with macrophage infiltration	Decrease DNA homologous recombination repair rate; Enhance cellular sensitivity to drugs	[49–51]
<i>Ferredoxin reductase (FDXR)</i>	A mitochondrial flavoprotein; Inhibiting iron homeostasis in tumor cells through the FDXR-P53 loop, leading to the suppression of tumor proliferation. Be implicated in the regulation of TP53 gene expression	Lower than normal tissues	It is higher than LGSOC in HGSOC	Closely associated with a favorable prognosis in ovarian cancer in terms of PFS and OS.	Positively correlated with tumor purity; Not significantly correlate with the infiltration of several immune cell types	Inhibited mutant TP53 expression and iron metabolism in cancer cells	[52–54]

**TABLE 1. Continued.**

Gene	Molecular functions	Expression levels compared to normal tissue	Expression levels in different subtypes	Association with ovarian cancer prognosis	Immune infiltration	Defect	Reference
<i>Epidermal growth factor receptor (EGFR)</i>	A transmembrane receptor; Mediates signal transduction with tyrosine kinase activity; Upon ligand binding, EGFR can activate various signaling pathways, leading to cancer cell proliferation, migration, and invasion	Lower than normal tissues	It is higher than LGSOC in HGSOC	Associated with poor prognosis of PFS of ovarian cancer	Negatively correlated with tumor purity; Not significantly correlate with the infiltration of several immune cell types	Preventing the metastasis of ovarian cancer cells	[55–59]
<i>C-X-C motif chemokine ligand 11/interferon-inducible T-cell alpha chemoattractant (CXCL11/I-TAC)</i>	A chemokine	Higher than normal tissues	It is higher than HGSOC in LGSOC	Closely associated with a favorable prognosis in ovarian cancer in terms of OS	Negatively correlated with tumor purity; Significant positive correlations with B cells, CD8+ T cells, cluster of differentiation 4 positive (CD4+) T cells, macrophage, neutrophil and DC cell infiltration		[60]

However, paradoxically, the expression of *TP53* in ovarian cancer tissues was higher than in normal tissues, and its content was significantly higher in HGSOC than in LGSOC. Notably, although *TP53* was more abundant in HGSOC, the mutation rate of this gene in HGSOC exceeded 90%, whereas it was less than 10% in LGSOC [46]. The accumulation of mutant *TP53* has been linked to multidrug resistance in ovarian cancer and an increased probability of cancer cell metastasis to the abdominal cavity [46, 47]. Therefore, it is plausible that the high expression of this mutant *TP53* may contribute to the poor prognosis of ovarian cancer. In addition, our findings revealed that *TP53* expression was higher in advanced ovarian cancer patients, and LGSOC tended to occur in younger patients compared to HGSOC [48], which might explain the lower expression of *TP53* in LGSOC. Our research also indicated an interaction between *TP53* and zinc, AZD 3355 and other drugs, providing a basis for the development of *TP53*-related targets and drug screening in ovarian cancer treatment. TP53I3, also known as p53 inducible gene 3 (PIG3), is a reactive oxygen species inducer that can be activated by the tumor suppressor TP53 [49, 50]. Studies have reported that the absence of TP53I3 can decrease DNA homologous recombination repair rate, resulting in genome instability and increased susceptibility to cancer development. Additionally, the absence of TP53I3 can enhance cellular sensitivity to drugs [50, 51]. Our results also demonstrated that high *TP53I3* expression was closely associated with a favorable prognosis in ovarian cancer in terms of PFS and OS. However, the expression of *TP53I3* in cancer tissues was higher than in normal tissues, potentially due to transcriptional activation by TP53 [50]. Similar to *TP53*, *TP53I3* expression increased with the age of ovarian cancer patients, and its content was significantly higher in HGSOC compared to LGSOC. These findings suggest a possible correlation between LGSOC's tendency to occur in younger patients and the expression of *TP53I3*.

Studies have demonstrated that ferredoxin reductase (FDXR), a mitochondrial flavoprotein, plays a role in inhibiting iron homeostasis in tumor cells through the FDXR-P53 loop, leading to the suppression of tumor proliferation. FDXR is also implicated in the regulation of *TP53* gene expression and has been identified as a target of TP53 [52–54]. Our study found that high FDXR expression was closely associated with a favorable prognosis in ovarian cancer, and the expression level of *FDXR* in ovarian cancer tissue was lower than that in normal tissue. Additionally, the expression level in high-grade serous ovarian cancer (HGSOC) was higher than in low-grade serous ovarian cancer (LGSOC), suggesting the existence of a regulatory loop between FDXR and TP53. FDXR was required for both wild-type and mutant *TP53* expression, although a loss of FDXR inhibited mutant *TP53* expression and iron metabolism in cancer cells, but not wild-type *TP53* [52, 54]. The feedback regulation of the FDXR-P53 loop might contribute to the higher expression of *FDXR* in HGSOC. As previously stated, the mutation rate of *TP53* in HGSOC exceeds 90%. Our study revealed that *FDXR* can be targeted by Flavin adenine dinucleotide and 2'-monophosphoadenosine 5'-diphosphoribose. Thus, targeting *FDXR* may offer a promising approach for the treatment of HGSOC. Epidermal growth factor receptor (EGFR) is a

transmembrane receptor that mediates signal transduction with tyrosine kinase activity [55]. Our results indicated that EGFR was associated with poor prognosis in ovarian cancer. Upon ligand binding, EGFR can activate various signaling pathways, such as PI3K/Akt, mitogen-activated protein kinase/Extracellular signal-regulated kinase (MAPK/ERK) and signal transducer and activator of transcription (STAT) signaling pathways, leading to cancer cell proliferation, migration and invasion [56]. miR-7 has been shown to target EGFR and inhibit the function of the EGFR pathway, thus preventing the metastasis of ovarian cancer cells [57]. The expression of *EGFR* in HGSOC was higher than that in LGSOC, which may also contribute to the shorter overall survival of HGSOC. Among these five hub genes, *EGFR* interacts with more drugs, and abnormal activation of *EGFR* has been closely linked to the poor prognosis of ovarian cancer patients [58, 59]. Therefore, the development of therapeutic strategies targeting EGFR remains an important area of research.

CXCL11, also known as T-cell alpha chemokine (I-TAC), is primarily induced by interferon  $\gamma$  and IFN- $\beta$  (interferon-beta) [60, 61] and is mainly produced by macrophages [62]. CXCL11 plays a role in the progression of various cancers. Studies have shown that *CXCL11* is highly expressed in colon cancer tissues compared to normal tissues and is associated with prolonged survival [63, 64]. Similarly, in breast cancer tissues, *CXCL11* is also highly expressed and has been implicated in promoting breast cancer development [65]. Consistent with the findings of Furuya *et al.* [62], our study demonstrated that *CXCL11* was significantly upregulated in tumor tissues compared to normal tissues. CXCL11 has also been identified as a predictive marker for ovarian cancer clinical outcomes [60]. Our analysis revealed a significantly higher expression of *CXCL11* in LGSOC than in HGSOC, and the OS results showed that high *CXCL11* expression was closely associated with a favorable prognosis in ovarian cancer, which could be one of the reasons for the better prognosis of LGSOC compared to HGSOC. However, there may be certain potential limitations in our study. Firstly, the data relied on two gene expression profiles (GSE27651 and GSE73168) from the GEO database, which may introduce sample source inconsistencies and potential biases. Secondly, while bioinformatics methods were used for data analysis, the functional analysis focused on enriched KEGG pathways related to HGSOC and LGSOC but lacked in-depth exploration of their roles in cancer development and treatment, as well as their impact on specific therapeutic targets. These limitations highlight the need for further research.

## 5. Conclusions

In conclusion, this study utilized bioinformatics analysis to examine the enrichment of DEGs in HGSOC and LGSOC and revealed promising key hub genes. The findings contribute to a better understanding of the distinctions between LGSOC and HGSOC and provide a foundation for future research to further explore these differences, which could help improve the treatments and outcomes of patients with ovarian cancer.

## AVAILABILITY OF DATA AND MATERIALS

The data generated in the present study may be requested from the corresponding author. For publicly available datasets, the data generated in the present study may be found in the GEO database.

## AUTHOR CONTRIBUTIONS

YG, JHC—conceptualization, supervision, writing-review & editing. KM, YXZ, YMQ—data curation. KM, YG—funding acquisition. KM, YXZ, YMQ, CQL—investigation. KM—project administration, visualization; KM, JHC—resources. KM, MMY, ZMZ—software. YG—validation. KM, YXZ, JYZ—writing-original draft.

## ETHICS APPROVAL AND CONSENT TO PARTICIPATE

Not applicable.

## ACKNOWLEDGMENT

Not applicable.

## FUNDING

This research was funded by “Research Fund for Lin He’s Academician Workstation of New Medicine and Clinical Translation in Jining Medical University, grant number JYHL2021MS13” and “Teachers Research Support Fund in Jining Medical University, grant number JYFC2019KJ001”.

## CONFLICT OF INTEREST

The authors declare no conflict of interest.

## REFERENCES

- [1] Ma H, Tian T, Cui Z. Targeting ovarian cancer stem cells: a new way out. *Stem Cell Research & Therapy*. 2023; 14: 28.
- [2] Lu W, Xie B, Tan G, Dai W, Ren J, Pervaz S, *et al*. Elafin is related to immune infiltration and could predict the poor prognosis in ovarian cancer. *Frontiers in Endocrinology*. 2023; 14: 1088944.
- [3] Allemani C, Matsuda T, Di Carlo V, Harewood R, Matz M, Nikšić M, *et al*. Global surveillance of trends in cancer survival 2000–14 (CONCORD-3): analysis of individual records for 37 513 025 patients diagnosed with one of 18 cancers from 322 population-based registries in 71 countries. *The Lancet*. 2018; 391: 1023–1075.
- [4] Miller DS, Blessing JA, Krasner CN, Mannel RS, Hanjani P, Pearl ML, *et al*. Phase II evaluation of pemetrexed in the treatment of recurrent or persistent platinum-resistant ovarian or primary peritoneal carcinoma: a study of the Gynecologic Oncology Group. *Journal of Clinical Oncology*. 2009; 27: 2686–2691.
- [5] Beaver JA, Coleman RL, Arend RC, Armstrong DK, Bala S, Mills GB, *et al*. Advancing drug development in gynecologic malignancies. *Clinical Cancer Research*. 2019; 25: 4874–4880.
- [6] Lu H, Liu Y, Wang J, Fu S, Wang L, Huang C, *et al*. Detection of ovarian cancer using plasma cell-free DNA methylomes. *Clinical Epigenetics*. 2022; 14: 74.
- [7] Lim MC, Chang SJ, Park B, Yoo HJ, Yoo CW, Nam BH, *et al*. Survival after hyperthermic intraperitoneal chemotherapy and primary or interval cytoreductive surgery in ovarian cancer: a randomized clinical trial. *JAMA Surgery*. 2022; 157: 374–383.
- [8] Gershenson DM. Low-grade serous carcinoma of the ovary or peritoneum. *Annals of Oncology*. 2016; 27: i45–i49.
- [9] Barnes BM, Nelson L, Tighe A, Burghel GJ, Lin I, Desai S, *et al*. Distinct transcriptional programs stratify ovarian cancer cell lines into the five major histological subtypes. *Genome Medicine*. 2021; 13: 140.
- [10] Bartoletti M, Musacchio L, Giannone G, Tuninetti V, Bergamini A, Scambia G, *et al*. Emerging molecular alterations leading to histology-specific targeted therapies in ovarian cancer beyond PARP inhibitors. *Cancer Treatment Reviews*. 2021; 101: 102298.
- [11] Kaldawy A, Segev Y, Lavie O, Auslender R, Sopik V, Narod SA. Low-grade serous ovarian cancer: a review. *Gynecologic Oncology*. 2016; 143: 433–438.
- [12] Bussies PL, Schlumbrecht M. Dual fulvestrant-trametinib therapy in recurrent low-grade serous ovarian cancer. *The Oncologist*. 2020; 25: e1124–e1126.
- [13] King ER, Tung CS, Tsang YTM, Zu Z, Lok GTM, Deavers MT, *et al*. The anterior gradient homolog 3 (AGR3) gene is associated with differentiation and survival in ovarian cancer. *American Journal of Surgical Pathology*. 2011; 35: 904–912.
- [14] Gao Q, Yang Z, Xu S, Li X, Yang X, Jin P, *et al*. Correction: heterotypic CAF-tumor spheroids promote early peritoneal metastasis of ovarian cancer. *Journal of Experimental Medicine*. 2019; 216: 2448.
- [15] Zhou Y, Zhou B, Pache L, Chang M, Khodabakhshi AH, Tanaseichuk O, *et al*. Metascape provides a biologist-oriented resource for the analysis of systems-level datasets. *Nature Communications*. 2019; 10: 1523.
- [16] Meng K, Cao J, Dong Y, Zhang M, Ji C, Wang X. Application of bioinformatics analysis to identify important pathways and hub genes in ovarian cancer affected by WT1. *Frontiers in Bioengineering and Biotechnology*. 2021; 9: 741051.
- [17] Bu D, Luo H, Huo P, Wang Z, Zhang S, He Z, *et al*. KOBAS-i: intelligent prioritization and exploratory visualization of biological functions for gene enrichment analysis. *Nucleic Acids Research*. 2021; 49: W317–W325.
- [18] Szklarczyk D, Kirsch R, Koutrouli M, Nastou K, Mehryary F, Hachilif R, *et al*. The STRING database in 2023: protein–protein association networks and functional enrichment analyses for any sequenced genome of interest. *Nucleic Acids Research*. 2023; 51: D638–D646.
- [19] Shannon P, Markiel A, Ozier O, Baliga NS, Wang JT, Ramage D, *et al*. Cytoscape: a software environment for integrated models of biomolecular interaction networks. *Genome Research*. 2003; 13: 2498–2504.
- [20] Hoadley KA, Yau C, Hinoue T, Wolf DM, Lazar AJ, Drill E, *et al*. Cell-of-origin patterns dominate the molecular classification of 10,000 tumors from 33 types of cancer. *Cell*. 2018; 173: 291–304.e6.
- [21] Tang Z, Li C, Kang B, Gao G, Li C, Zhang Z. GEPIA: a web server for cancer and normal gene expression profiling and interactive analyses. *Nucleic Acids Research*. 2017; 45: W98–W102.
- [22] Gyorffy B, Lániczky A, Szállási Z. Implementing an online tool for genome-wide validation of survival-associated biomarkers in ovarian-cancer using microarray data from 1287 patients. *Endocrine-Related Cancer*. 2012; 19: 197–208.
- [23] Györfy B. Discovery and ranking of the most robust prognostic biomarkers in serous ovarian cancer. *GeroScience*. 2023; 45: 1889–1898.
- [24] Li T, Fan J, Wang B, Traugh N, Chen Q, Liu JS, *et al*. TIMER: a web server for comprehensive analysis of tumor-infiltrating immune cells. *Cancer Research*. 2017; 77: e108–e110.
- [25] Chandrashekar DS, Karthikeyan SK, Korla PK, Patel H, Shovon AR, Athar M, *et al*. UALCAN: an update to the integrated cancer data analysis platform. *Neoplasia*. 2022; 25: 18–27.
- [26] Ru B, Wong CN, Tong Y, Zhong JY, Zhong SSW, Wu WC, *et al*. TISIDB: an integrated repository portal for tumor-immune system interactions. *Bioinformatics*. 2019; 35: 4200–4202.
- [27] Chang L, Xia J. MicroRNA regulatory network analysis using miRNet 2.0. *Transcription Factor Regulatory Networks*. 2023; 146: 185–204.
- [28] Sallum LF, Andrade L, Bastos Eloy da Costa L, Ramalho S, Ferracini AC, Natal RDA, *et al*. BRCA1, Ki67, and  $\beta$ -Catenin immunoeexpression is not related to differentiation, platinum response, or prognosis in women with low- and high-grade serous ovarian carcinoma. *International Journal of Gynecologic Cancer*. 2018; 28: 437–447.

- [29] Kang JH, Lai YL, Cheng WF, Kim HS, Kuo KT, Chen YL, *et al.* Clinical factors associated with prognosis in low-grade serous ovarian carcinoma: experiences at two large academic institutions in Korea and Taiwan. *Scientific Reports*. 2020; 10: 20012.
- [30] Goulding EA, Simcock B, McLachlan J, van der Griend R, Sykes P. Low-grade serous ovarian carcinoma: a comprehensive literature review. *Australian and New Zealand Journal of Obstetrics and Gynaecology*. 2020; 60: 27–33.
- [31] Romero I, Leskelä S, Mies BP, Velasco AP, Palacios J. Morphological and molecular heterogeneity of epithelial ovarian cancer: therapeutic implications. *European Journal of Cancer Supplements*. 2020; 15: 1–15.
- [32] Huang J. Current developments of targeting the p53 signaling pathway for cancer treatment. *Pharmacology & Therapeutics*. 2021; 220: 107720.
- [33] Li H, Zeng Z, Yang X, Chen Y, He L, Wan T. LncRNA GClnc1 may contribute to the progression of ovarian cancer by regulating p53 signaling pathway. *European Journal of Histochemistry*. 2020; 64: 3166.
- [34] Golubovskaya VM, Kweh FA, Cance WG. Focal adhesion kinase and cancer. *Histology & Histopathology*. 2009; 24: 503–510.
- [35] Tai Y, Chen L, Shen T. Emerging roles of focal adhesion kinase in cancer. *BioMed Research International*. 2015; 2015: 690690.
- [36] Revach O, Grosheva I, Geiger B. Biomechanical regulation of focal adhesion and invadopodia formation. *Journal of Cell Science*. 2020; 133: jcs244848.
- [37] Chen L, Qian J, You Q, Ma J. LIM domain-containing 2 (LIMD2) promotes the progress of ovarian cancer *via* the focal adhesion signaling pathway. *Bioengineered*. 2021; 12: 10089–10100.
- [38] Nolasco-Quiroga M, Rosas-Díaz M, Moreno J, Godínez-Aguilar R, López-Ibarra MJ, Piña-Sánchez P, *et al.* Increased expression of FAK isoforms as potential cancer biomarkers in ovarian cancer. *Oncology Letters*. 2019; 17: 4779–4786.
- [39] Mitra AK, Sawada K, Tiwari P, Mui K, Gwin K, Lengyel E. Ligand-independent activation of c-Met by fibronectin and  $\alpha(5)\beta(1)$ -integrin regulates ovarian cancer invasion and metastasis. *Oncogene*. 2011; 30: 1566–1576.
- [40] Chen C, Shyu M, Wang S, Chou C, Huang M, Lin T, *et al.* MUC20 promotes aggressive phenotypes of epithelial ovarian cancer cells *via* activation of the integrin  $\beta 1$  pathway. *Gynecologic Oncology*. 2016; 140: 131–137.
- [41] Huang H, Lin Y, Chang H, Lai Y, Chen Y, Huang S, *et al.* Chemoresistant ovarian cancer enhances its migration abilities by increasing store-operated  $\text{Ca}^{2+}$  entry-mediated turnover of focal adhesions. *Journal of Biomedical Science*. 2020; 27: 36.
- [42] Xu X, Chen F, Zhang L, Liu L, Zhang C, Zhang Z, *et al.* Exploring the mechanisms of anti-ovarian cancer of *Hedyotis diffusa willd* and *Scutellaria barbata D. Don* through focal adhesion pathway. *Journal of Ethnopharmacology*. 2021; 279: 114343.
- [43] Balkwill FR. The chemokine system and cancer. *The Journal of Pathology*. 2012; 226: 148–157.
- [44] Goenka A, Khan F, Verma B, Sinha P, Dmello CC, Jogalekar MP, *et al.* Tumor microenvironment signaling and therapeutics in cancer progression. *Cancer Communications*. 2023; 43: 525–561.
- [45] Morein D, Erlichman N, Ben-Baruch A. Beyond cell motility: the expanding roles of chemokines and their receptors in malignancy. *Frontiers in Immunology*. 2020; 11: 952.
- [46] Guo T, Dong X, Xie S, Zhang L, Zeng P, Zhang L. Cellular mechanism of gene mutations and potential therapeutic targets in ovarian cancer. *Cancer Management and Research*. 2021; 13: 3081–3100.
- [47] Zhang M, Zhuang G, Sun X, Shen Y, Wang W, Li Q, *et al.* TP53 mutation-mediated genomic instability induces the evolution of chemoresistance and recurrence in epithelial ovarian cancer. *Diagnostic Pathology*. 2017; 12: 16.
- [48] Chen M, Jin Y, Bi Y, Yin J, Wang Y, Pan L. A survival analysis comparing women with ovarian low-grade serous carcinoma to those with high-grade histology. *OncoTargets and Therapy*. 2014; 7: 1891–1899.
- [49] Zhang W, Luo J, Chen F, Yang F, Song W, Zhu A, *et al.* BRCA1 regulates PIG3-mediated apoptosis in a p53-dependent manner. *Oncotarget*. 2015; 6: 7608–7618.
- [50] Chaudhry SR, Lopes J, Levin NK, Kalpage H, Tainsky MA. Germline mutations in apoptosis pathway genes in ovarian cancer; the functional role of a TP53I3 (PIG3) variant in ROS production and DNA repair. *Cell Death Discovery*. 2021; 7: 62.
- [51] Lopes JL, Chaudhry S, Lopes GS, Levin NK, Tainsky MA. FANCM, RAD1, CHEK1 and TP53i3 act as BRCA-like tumor suppressors and are mutated in hereditary ovarian cancer. *Cancer Genetics*. 2019; 235–236: 57–64.
- [52] Zhang Y, Feng X, Zhang J, Chen M, Huang E, Chen X. Iron regulatory protein 2 is a suppressor of mutant p53 in tumorigenesis. *Oncogene*. 2019; 38: 6256–6269.
- [53] Zhang Y, Qian Y, Zhang J, Yan W, Jung Y, Chen M, *et al.* Ferredoxin reductase is critical for p53-dependent tumor suppression *via* iron regulatory protein 2. *Genes & Development*. 2017; 31: 1243–1256.
- [54] Zhang J, Chen X. P53 tumor suppressor and iron homeostasis. *The FEBS Journal*. 2019; 286: 620–629.
- [55] Cai G, Zhu L, Chen X, Sun K, Liu C, Sen GC, *et al.* TRAF4 binds to the juxtamembrane region of EGFR directly and promotes kinase activation. *Proceedings of the National Academy of Sciences*. 2018; 115: 11531–11536.
- [56] Chuang TC, Wu K, Lin YY, Kuo HP, Kao MC, Wang V, *et al.* Dual down-regulation of EGFR and ErbB2 by berberine contributes to suppression of migration and invasion of human ovarian cancer cells. *Environmental Toxicology*. 2021; 36: 737–747.
- [57] Cui X, Song K, Lu X, Feng W, Di W. Liposomal delivery of MicroRNA-7 targeting EGFR to inhibit the growth, invasion, and migration of ovarian cancer. *ACS Omega*. 2021; 6: 11669–11678.
- [58] Zhao J, Tan W, Zhang L, Liu J, Shangguan M, Chen J, *et al.* FGFR3 phosphorylates EGFR to promote cisplatin-resistance in ovarian cancer. *Biochemical Pharmacology*. 2021; 190: 114536.
- [59] Zhang M, Cong Q, Zhang X, Zhang M, Lu Y, Xu C. Pyruvate dehydrogenase kinase 1 contributes to cisplatin resistance of ovarian cancer through EGFR activation. *Journal of Cellular Physiology*. 2019; 234: 6361–6370.
- [60] Jin C, Xue Y, Li Y, Bu H, Yu H, Zhang T, *et al.* A 2-protein signature predicting clinical outcome in high-grade serous ovarian cancer. *International Journal of Gynecologic Cancer*. 2018; 28: 51–58.
- [61] Rani MR, Foster GR, Leung S, Leaman D, Stark GR, Ransohoff RM. Characterization of beta-R1, a gene that is selectively induced by interferon beta (IFN-beta) compared with IFN-alpha. *Journal of Biological Chemistry*. 1996; 271: 22878–22884.
- [62] Furuya M, Suyama T, Usui H, Kasuya Y, Nishiyama M, Tanaka N, *et al.* Up-regulation of CXC chemokines and their receptors: implications for proinflammatory microenvironments of ovarian carcinomas and endometriosis. *Human Pathology*. 2007; 38: 1676–1687.
- [63] Cao Y, Jiao N, Sun T, Ma Y, Zhang X, Chen H, *et al.* CXCL11 correlates with antitumor immunity and an improved prognosis in colon cancer. *Frontiers in Cell and Developmental Biology*. 2021; 9: 646252.
- [64] Liu K, Lai M, Wang S, Zheng K, Xie S, Wang X. Construction of a CXC chemokine-based prediction model for the prognosis of colon cancer. *BioMed Research International*. 2020; 2020: 6107865.
- [65] Zhang J, Hu D. miR-1298-5p influences the malignancy phenotypes of breast cancer cells by inhibiting CXCL11. *Cancer Management and Research*. 2021; 13: 133–145.

**How to cite this article:** Kai Meng, Yixin Zhang, Yuanmin Qi, Chuqi Liu, Mengmeng Yao, Zhimin Zhang, *et al.* Identification of differential molecular characteristics and key genes between low- and high-grade serous ovarian cancer by bioinformatics analysis. *European Journal of Gynaecological Oncology*. 2025; 46(1): 47–62. doi: 10.22514/ejgo.2025.006.